

# Electronic Structure Simulation of Aluminum Antimony Nanocrystal Using Ab-initio Density Functional Theory coupled with Large Unit Cell Method

Akram Hashim Taha

Physics Dept., Faculty of Science and Health, Koya University, Erbil, Iraq

**Abstract** Ab-initio density functional theory (DFT) calculations coupled with large unit cell method (LUC) and using generalized gradient approximation (GGA) were carried out to simulate the electronic structure of AlSb nanocrystal for 8, 16, 54 and 64 core atoms. Results show that the size of the core atoms affects the electronic properties for a limited value of number of core atoms then most properties tend to behave more stable. The energy gap, lattice constant and total energy are inversely proportional with the number of core atoms. Significant results occurred that the energy gap of aluminum antimony nanocrystal drops to a very small value (0.03) eV at 54 core atoms and this amount of energy is in the range of conductor materials. The density of states increased with increasing of number of core atoms.

**Keywords** Density Functional theory, AlSb nanocrystals, Large unit cell, Ab-initio

## 1. Introduction

Semiconductor nanocrystals of III-V compounds are of great significance due to their applications in various electronic and optical devices [1]. Rapid advances that have occurred in the preparation and characterization of nanocrystals, finally enable the studies of transformations between stable states of finite systems. Aluminum antimony (AlSb) seems to be a promising candidate for transistors and p-n junction diodes due to large band gap [2]. AlSb nanoclusters have also been synthesized by nanoscale electro deposition [3-5].

Aluminum antimony (AlSb) has been ranked as one of the most promising materials for detection of  $\gamma$ -ray radiation at or near ambient temperatures [6]. Yee et al. [7] concluded that at room temperature AlSb should make an intrinsically better high-energy photon detector than CdTe, Si, and Ge. Applications with particular interest in such detectors include the interception and assessment of nuclear material in the field; nuclear-weapon control and disarmament (material protection, control, and accounting); the monitoring of nuclear-material processing; dismantling nuclear weapons; and remote unattended monitoring [8]. GaAs and InP both suffer from limited or inaccessible supplies of Ga and in thereby making the large-scale implementation of large arrays impossible. In considering

materials availability, Al is one of the more abundant elements in the earth's crust. Sb, while less abundant, is still considered common and is more abundant than As, Be, Bi, Cd, Te, and W. AlSb was originally a material system of great interest because of its potential applications in electronic and photonic devices at high temperatures such as transistors, p-n junction diodes [7, 9, 10] and photovoltaic cells [6, 11, 12]. However, AlSb-based technologies never made any progress due to poor quality of surfaces that inhibit device processing and application. AlSb rapidly oxidizes when exposed to air, the growth of epitaxial layers and devices on AlSb substrates very difficult. Hence development of suitable chemical treatment of the wafer surface is crucial.

AlSb crystal is used in a multitude of device applications, including light-emitting diodes (LEDs), lasers, detectors, and communication devices. It is also a fabulous optical material, where it can be made to emit light efficiently, convert light energy into electrical energy, modulate the intensity of light and used as optical filters, mirrors, lenses, etc. [13]. Structural Phase Transition and the structural stability of nm sized AlSb nanocrystal in its zinc blende (B3), rocksalt (B1) and CsCl (B2) type phases under high compression of AlSb Nanocrystal has been investigated by Neha *et al.* using density functional theory [14].

Haider *et al.* studied the AlSb nanocrystals using restricted Hartree-Fock method [15]. In the present work we have used density functional theory formalism coupling with large unit cell method to investigate the electronic properties for AlSb nanocrystal for core atoms 8, 16, 54 and 64. The Slater Type Orbitals (STO) basis set is used in the

\* Corresponding author:

shahad246@yahoo.com (Akram Hashim Taha)

Published online at <http://journal.sapub.org/ajcmp>

Copyright © 2014 Scientific & Academic Publishing. All Rights Reserved

calculation besides we have used unrestricted Hartree-Fock formalism. These calculations were carried out using the Gaussian 03 software package [16].

## 2. Theory

The Schrödinger equation for one particle system can be solved simply, but it becomes more complicated for systems containing many particles. One of the most important goals of physics is to describe the physical properties of interacting many-particle systems. Such derivation requires the solution of the Schrödinger equation in  $3N$  spatial variables and  $N$  spin variables.

The Schrödinger equation of many body systems can be given by

$$\begin{aligned} \hat{H} \Psi(R_1, R_2, \dots, R_N, r_1, r_2, \dots, r_n) \\ = E \Psi(R_1, R_2, \dots, R_N, r_1, r_2, \dots, r_n) \end{aligned} \quad (1)$$

The Hamiltonian for a system containing  $n$  electrons and  $N$  nuclei.

$$\hat{H} = -\frac{1}{2} \sum_I \nabla_I^2 - \frac{1}{2} \sum_i \nabla_i^2 - \sum_i \sum_I \frac{Z_I}{r_{Ii}} + \sum_{I>J} \frac{Z_I Z_J}{r_{IJ}} + \sum_{i<j} \frac{1}{r_{ij}} \quad (2)$$

The most common ab-initio calculations is LCAO based. That is, the MO's are written as linear combination of the atomic basis set orbitals. ab-initio offers a variety of basis set such as Slater Type Orbitals (STOs) [17]. These wave functions are expressed in spherical polar coordinates to be [18, 19]:

$$\varphi_{n,l,m_l} = R_{nl}(r) Y_{lm}(\theta, \phi) \quad (3)$$

$n, l, m_l$  are the principal, azimuthal, and magnetic quantum numbers, respectively.

The radial nodes, in practice, make little difference to the description of bounding, but considerably complicated the calculation of electron-electron repulsion integrals. Slater proposed a series of radial functions lacking nodes [20]:

$$R_{nl}(r) = (2\zeta)^{\frac{n+1}{2}} \frac{1}{2} [(2n)!]^{-\frac{1}{2}} r^{n-1} e^{-\zeta r} \quad (4)$$

where

$$\zeta = \frac{Z-S}{n^*}$$

$Z$  is the atomic number,  $S$  is shielding parameter and  $n^* =$  effective principal quantum number the shielding parameter  $S$  is given an empirical value based on  $n$  and  $l$ . The radial function generates a set of atomic orbital-like basis functions, in combination with the angular functions that have subsequently become known as Slater-type orbitals (STOs).

Several theories gave approximate solutions to calculate the electronic structure, one of these powerful theories is the density functional theory (DFT). It gives a superior accuracy to Hartree-Fock theory, ab-initio and the semi-empirical

approaches. DFT is applicable from atoms, molecules containing heavy atoms and solids to nuclei, quantum and classical fluids [21, 22].

The central quantity in DFT is the electron density  $\rho(\mathbf{r})$ . It is defined as the integral over the spin coordinates of all electrons and over all but one of the spatial variables ( $\mathbf{x}=\mathbf{r},s$ ):

$$\rho(\vec{r}) = N \int \dots \int |\psi(\bar{x}_1, \bar{x}_2, \dots, \bar{x}_N)|^2 ds_1 d\bar{x}_2 \dots d\bar{x}_N \quad (5)$$

Where  $\rho(\mathbf{r})$  is the probability of finding any of the  $N$  electrons within a volume element  $d\mathbf{r}$ . Because  $\rho(\mathbf{r})$  represents the probability, this means that  $\rho(\mathbf{r})$  is a non-negative function and vanishes at infinity and integrates to the total number of electrons  $N$ .

The concept of DFT was put by Thomas-Fermi (1927) which is based on the uniform electron gas [23]. They proposed the following functional for the kinetic energy:

$$T_{TF}[\rho(\vec{r})] = \frac{3}{10} (2\pi^2) \int \rho^{5/3}(\vec{r}) d\vec{r} \quad (6)$$

Then, the energy can be given completely in terms of the electron density  $\rho(\vec{r})$  by using the classical expression for the nuclear-nuclear potential and electron-electron potential:

$$\begin{aligned} E_{TF}[\rho(\vec{r})] = \frac{3}{10} ((2\pi^2) \int \rho^{5/3}(\vec{r}) d\vec{r} - z \int \frac{\rho(\vec{r})}{r} d\vec{r} \\ + \frac{1}{2} \iint \frac{\rho(\vec{r}_1) \rho(\vec{r}_2)}{r_{12}} d\vec{r}_1 d\vec{r}_2 \end{aligned} \quad (7)$$

The initial work on density functional theory was reported in two publications: the first with Pierre Hohenberg (Hohenberg and Kohn, 1964) [24], and the second with Lu J. Sham (Kohn and Sham, 1965) [25]. Hohenberg and Kohn made the DFT possible by two ingeniously simple theories:

The first theorem states that "the external potential  $V_{\text{ext}}(\mathbf{r})$  for any interacting particles is a unique functional of the ground state density i.e.  $E = E[\rho(\vec{r})]$ . So the total energy can be written as:

$$E[\rho] = \int \rho(\vec{r}) V_{Ne}(\vec{r}) d\vec{r} + F_{HK}[\rho] \quad (8)$$

where

$$F_{HK}[\rho] = T[\rho] + E_{ee} \quad (9)$$

$F_{HK}[\rho]$  is a universal functional of  $\rho$ . The second theorem of Hohenberg-Kohn states "F<sub>HK</sub>[ $\rho$ ], the functional that delivers the ground state energy of the system, delivers the lowest energy if and only if the input density is the true ground state density" i.e.,

$$E_0 \leq E[\tilde{\rho}] = T[\tilde{\rho}] + E_{NE}[\tilde{\rho}] + E_{ee}[\tilde{\rho}] \quad (10)$$

It means that for any trial density  $\tilde{\rho}(\vec{r})$ , which satisfies the necessary boundary conditions such as  $\tilde{\rho}(\vec{r}) \geq 0$ ,  $\int \tilde{\rho}(\vec{r}) d\vec{r} = N$ , and associated with some external potential  $\tilde{V}_{\text{ext}}(\vec{r})$ , the obtained energy from the functional of equation (7) represents the upper of the ground state energy  $E_0$ .

In 1965 Kohn-sham [26] derived two sets of differential equations enabling the ground state density  $\tilde{\rho}(\vec{r})$  to be found.

Kohn and Sham introduced the following separation of the functional  $F[\rho]$ :

$$F[\rho]=T_s[\rho]+J[\rho]+E_{xc}[\rho] \quad (11)$$

Where  $T_s$  do not equal to the true kinetic energy of the system, and  $E_{xc}$  is the exchange-correlation energy.

This exchange-correlation energy is the functional that contains everything that is unknown. Then the energy of the interacting system will be:

$$E[\rho]=T_s[\rho]+J[\rho]+E_{xc}[\rho]+E_{Ne}[\rho] \quad (12)$$

The  $E_{xc}[\rho]$  term has no explicit form, and the functional derivative of  $E_{xc}$  with respect to  $\rho$  gives the exchange-correlation potential *i.e.*:

$$V_{xc} = \frac{\delta E_{xc}}{\delta \rho} \quad (13)$$

In order to minimize the energy a condition for the orbitals  $\{\psi_i\}$  must be given, with the usual constraint  $\langle \psi_i | \psi_j \rangle = \delta_{ij}$  and using the variational principle we get the resulting equation which is known as Kohn-Sham equation:

$$\left[ -\frac{1}{2}\nabla^2 + \left\{ \int \frac{\rho(\vec{r}_2)}{r_{12}} d\vec{r}_2 + V_{xc}(\vec{r}_1) - \sum_A \frac{Z_A}{r_{1A}} \right\} \right] \psi_i = \epsilon_i \psi_i \quad (14)$$

The Kohn-Sham formalism solves the Schrodinger equation iteratively in a self-consistent field (SCF) fashion. SCF is needed because the Coulomb potential and the exchange-correlation potential are functional of the density which itself depends on the unknown orbitals.

### 3. Results and Discussion

The software used in the present work is the Gaussian 03 to simulate some of the properties of AISb nanocrystal such as the optimized lattice constant, total energy, energy gap, etc... The optimized value of 8, 16, 54 and 64 core atoms of AISb nanocrystal have been calculated to find the minimum value of total energy (ground state) of each of these core atoms. Figure (1) shows the variation of total energy with lattice constant. The minimum energy means that the equilibrium point has been reached. Decreasing the distance between atoms leads to a decrease in the total energy, when the atoms become nearer to each other, the repulsive force will be the dominant. While at large distances the attractive force is the dominant. Stability of AISb nanocrystal at equilibrium lattice constant is due to the equality of attractive and repulsive forces. Equilibrium lattice constant ( $a_{equ.}$ ) decreases as the number of core atoms increases. Results shows a good agreement with results recorded in Ref. [15]. For bulk AISb the lattice constant is (0.6235) nm [27]. The  $a_{equ.}$  for 8, 16, 54 and 64 AISb core atoms were (0.6125, 0.6095, 0.603 and 0.6 nm) respectively. It is clear that the AISb nanocrystal's lattice constant tends to be close to the bulk value at small core atom.

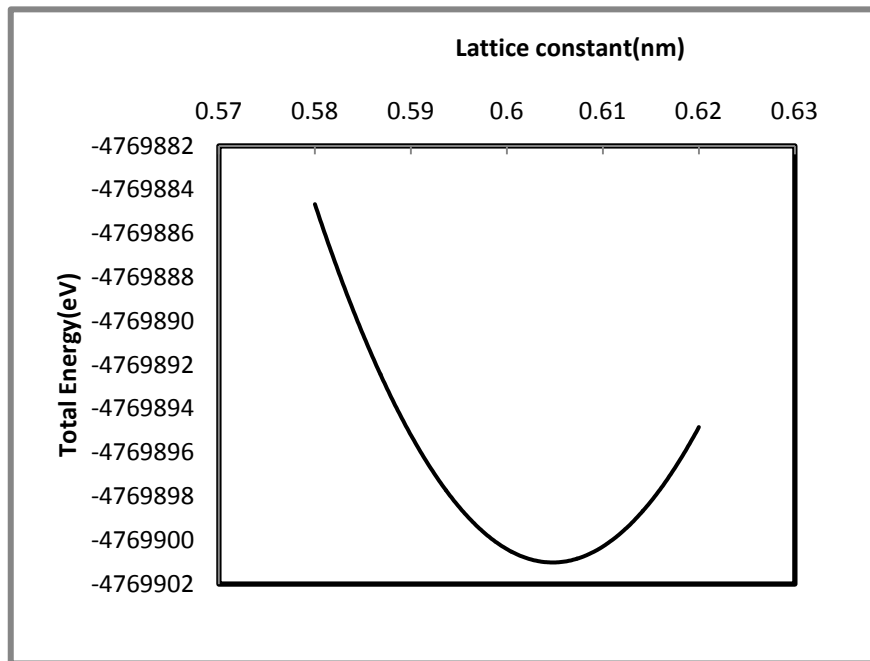


Figure 1. Shows the total energy variation with lattice constant of 54 core atoms of AISb nanocrystal

The total energy decreases with increasing the number of core atoms (Fig. 2). This is due to increasing of the binding energy when the number of atoms is increase.

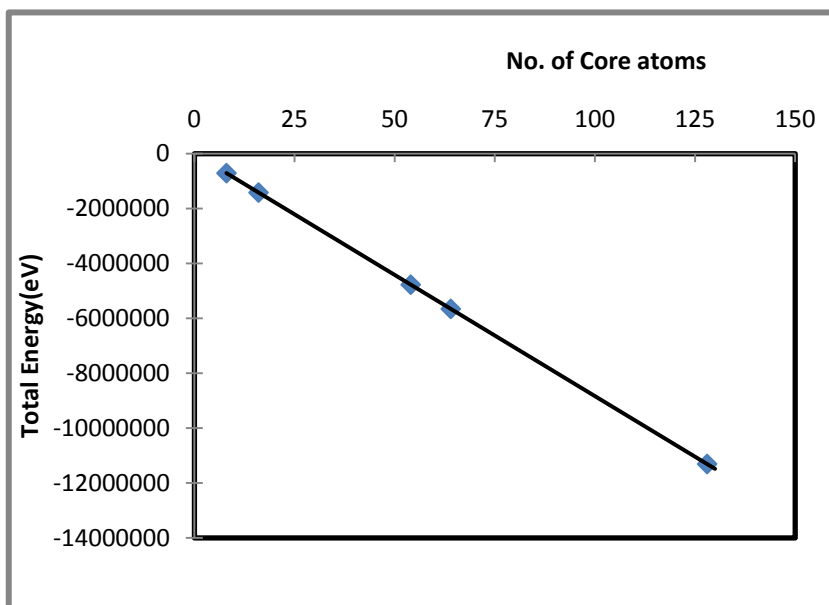


Figure 2. Shows the total energy as a function of number of core atoms for AlSb nanocrystal

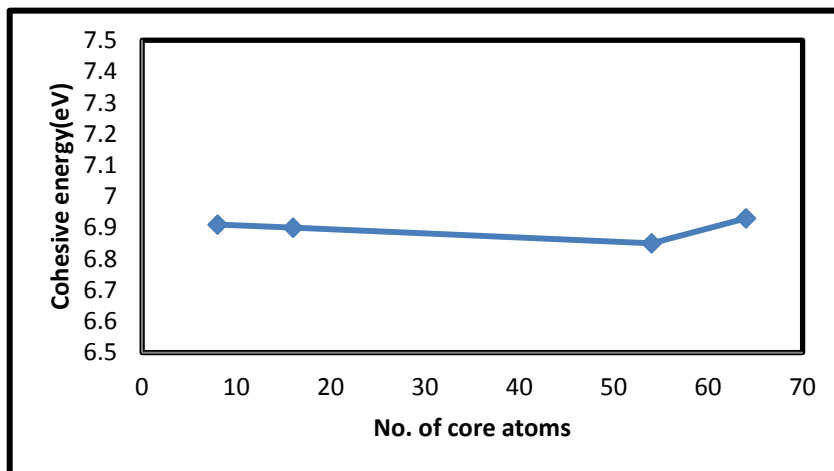


Figure 3. The variation of cohesive energy Vs the number of core atoms for AlSb nanocrystal

The cohesive energy has been calculated using the following equation [28]

$$E_{coh.} = \frac{E_T}{n} - E_{Free} - E_0$$

$E_{Free}$  is the experimental free atom energy,  $E_0$  represents the correction to the cohesive energy for the zero-point motion of the nuclei [29] the theoretical value of the cohesive energy of bulk AlSb is (8.08 eV) according to Ahmed, et al [30] and experimentally Wyckoff found it to be (6.60eV) [31], while Aresti and Verma found its experimental value to be (7.155 and 6.0245 eV) respectively [32, 33]. The calculated values in this work for AlSb nanocrystal for 8, 16, 54 and 64 core atoms was fluctuating about 6.90 eV see fig. (3).

Several studies indicated that the lattice constant decreases with increasing the number of core atoms [34].

The lattice constant decreases as the number of core atoms increase (fig. 4). The lattice constant for low values of number of core atoms converges to the value of the experimental bulk AlSb (6.136 nm) [35].

Fig.5 shows the (highest occupied molecular orbitals (HOMO) and lowest unoccupied molecular orbitals (LUMO) energies as a function of the number of core atoms. HOMO and LUMO orbitals shows shape effects. There is a continues fluctuated indefinitely as a result of the formation of different surfaces in larger nanocrystals [36]. Moreover, electric affinity, Fermi level and ionization are included in the HOMO and LUMO orbital energies. Fermi level is the average of LUMO and HOMO energies [37]. As a result of these relatives, the behavior for both HOMO and LUMO is approximately the same.

Fig. 6 gives the relationship between the energy gap and the number of core atoms. Remarkable behaviors occur in

this study that the energy gap tends to become too small when the number of core atoms becomes large. This is due to the increasing in the Al metal atoms, so the dominant is the

aluminum atoms in the AlSb nanocrystal. The AlSb nanocrystals at high core atom behaves like a conductor.

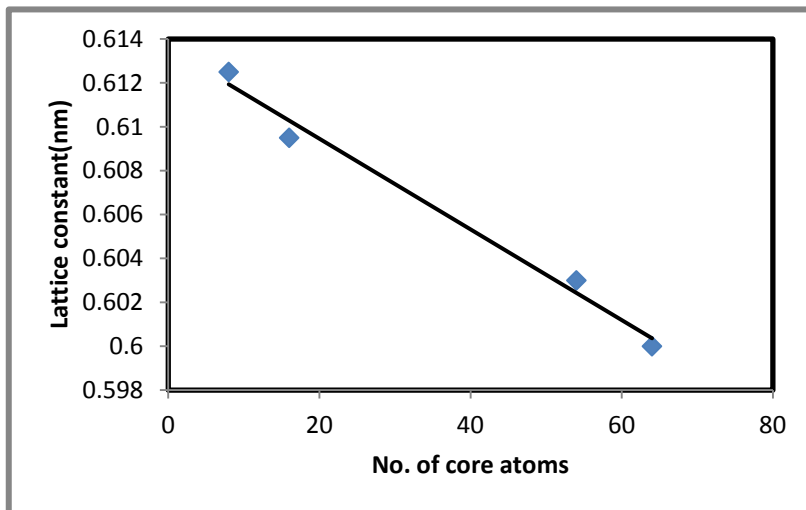


Figure 4. The variation of the lattice constant with the number of core atoms for LUC AlSb nanocrystal

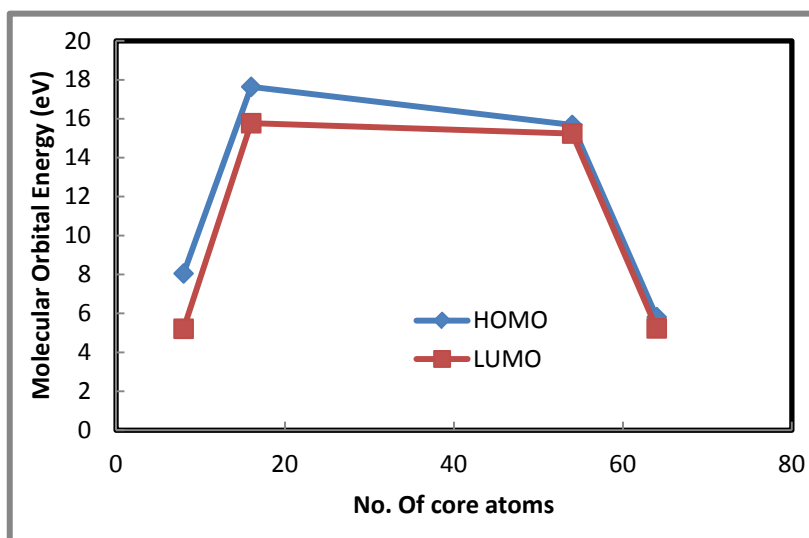


Figure 5. Shows the HOMO and LUMO as a function of number of core atoms for AlSb nanocrystal

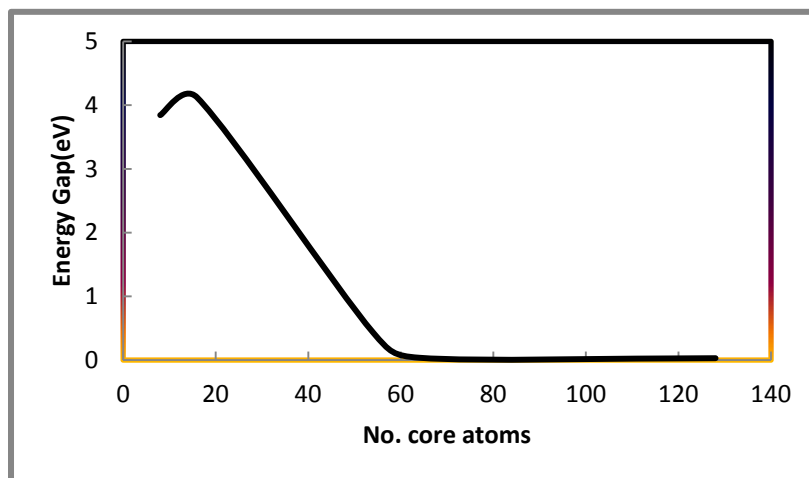


Figure 6. Shows the variation of energy gap with the number of core atoms for AlSb nanocrystal

The highest density of states as a function of number of core atoms is shown in Fig. (7). Linear dependency is obvious in the graph, increasing the LUC core atoms means generating more energy states. Density of state shaping if different between the nanocrystals and bulk materials due to the confinement effect (the quantum size effect on the electrons) [38]. This variation in the DOS between bulk and nanostructure effect is caused by the dependency of DOS on the energy, where for bulk materials the density of states is

proportional to  $E^{1/2}$ , while The density of states diverges as  $(E-E_{ij})^{-1/2}$  [39], Where  $E_{ij}$  is the subband energy state.

Finally the density of states for 8 and 64 LUC core atoms is shown in figures 8 and 9. The number of energy states for any specific energy value is increased gradually with increasing the number of core atoms. Also the energy levels seems to be nearer to each other as No. of core atoms increased.

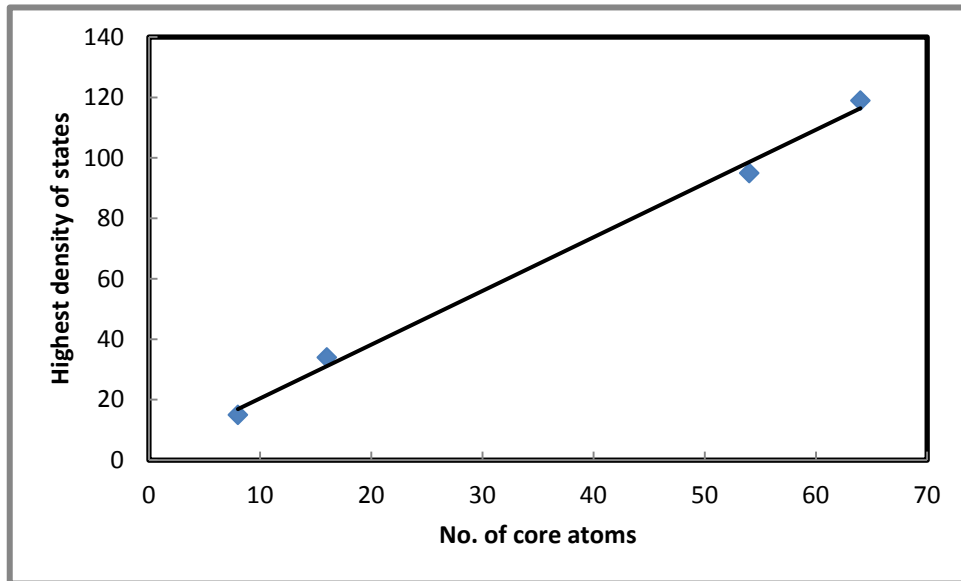


Figure 7. Shows the highest density of states as a function of number of core atoms for AlSb nanocrystals

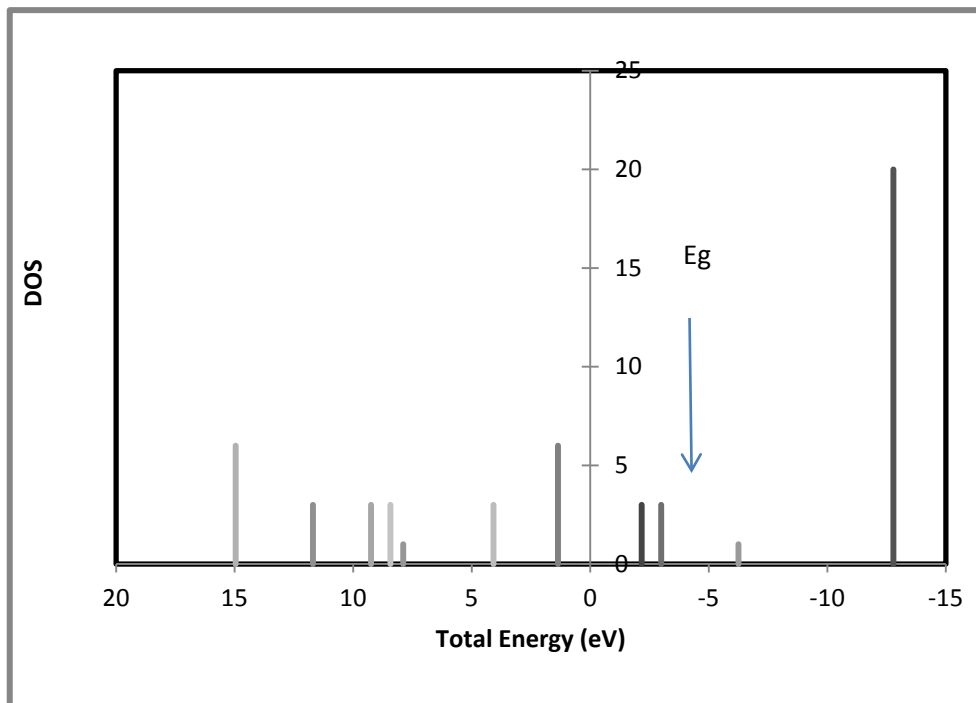


Figure 8. Shows the density of states Vs the total energy for 8 atoms AlSb nanocrystal

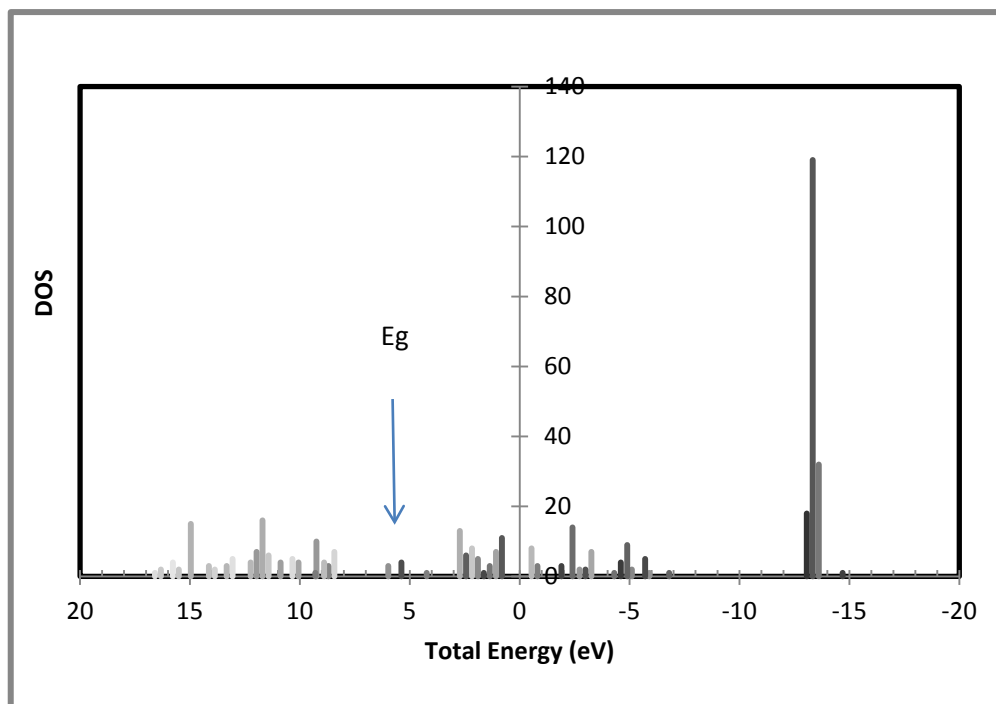


Figure 9. Shows the density of states Vs the total energy for 64 atoms AlSb nanocrystal

## 4. Conclusions

A remarkable results found in this study is that the AlSb nanocrystals have a significant properties than bulk AlSb material. Ab-initio using the Gaussian 03 software stimulates some of important properties of nanocrystals rather than bulk materials. In the present work we can conclude that, the total energy, lattice constant and the energy gap are inversely proportional with the number of LUC core atoms while the density of states is proportional to the number of core atoms. The cohesive energy showed a fluctuated value with respect to increasing the number of core atoms. No significant dependency shown in this study between  $E_{\text{coh}}$ . And the number of core atoms. Same behavior for both HOMO and LUMO with varying the number of core atoms.

## REFERENCES

- [1] A. H. Mueller, M. A. Petruska, M. Ac. Donald, J. Werder, E. A. Akhadov, D. D. Koleske, M. A. Hoffbauer and V. I. Klimov, Nano Letters, vol 5, May 2005, pp. 1039-1044.
- [2] H. R. R. Haberecht, and A. E. Middleton, J. Electrochem. Soc., vol 105, 1958, pp. 533-540.
- [3] Y. K. Noh, S. R. Park, M. D. Kim, Y. J. Kwon, J. E. Oh, Y. H. Kim, J.Y. Lee, S.G. Kim, K.S. Chung and T.G. Kim, J. Cryst. Growth, vol. 301, 2007, pp. 244-247.
- [4] C. L. Aravindaand W. Freyland, Chem. Commun., 2006, pp. 1703-1705.
- [5] S. H. Tolbert and A. P. Alivisatos, J. Science , vol. 265, 1994, pp. 373-376.
- [6] G.A. Armantrout, S.P. Swierkowski, J.W. Sherohman, J.H. Yee, IEEE Trans. Nucl. Sci. NS-24 (1977) 121.
- [7] J.H. Yee, S.P. Swierkoski, J.W. Sherohman, IEEE Trans. Nucl. Sci.NS-24 (1977) 1962.
- [8] John Sherohman, High-resistivity aluminum antimonide radiation detectors, Lawrence Livermore National Laboratory, website 2005, /http://rdc.llnl.gov/rdp/high\_resistency.htmlS.
- [9] A. Herczog, R.R. Haberecht, A.E. Middleton, J. Electrochem. Soc. 105 (1958) 533.
- [10] R.J. Stirn, W.M. Becker, Phys. Rev. 148 (1966) 907.
- [11] G.A. Armantrout, J.H Yee, AlSb as a potential photovoltaic material, Second E.C. Photovoltaic Solar Energy Conference: Proceedings of the International Conference, Berlin (West), 23–26 April 1979, pp. 960–967.
- [12] P. Becla, A.F. Witt, AlSb photonic detectors for gamma-rayspectroscopy, Progress Report DOE/NV/11627-T1, 1995.
- [13] D. Aberg, P. Erhart, A. J. Williamson and V. Lordi, Phys. Rev. B, Vol. 77, No. 16, 2008, pp. 165206-165216.
- [14] Neha Tyagi and Anurag Srivastava, International Conference: Nanoscience, Engineering and Technology (ICONSET) Sathyabama University, India, November 28th-30th, (2011), pp 421-423.
- [15] Haider I. Isa, Ahmed M. Abdul-Lettif, World Journal of Condensed Matter Physics, 2, 129-132 (2012).
- [16] Frisch, M.J., Trucks, G.W., Schlegel, H.B., et al.: Gaussian 03, Revision B.01, Gaussian, Inc., Pittsburgh, PA, 2003.
- [17] Slater, J. C., "Atomic Shielding Constants", Phys. Rev. 36, 57 (1930).
- [18] Roy Mc Weeny "Quantum mechanics of many-particle

- systems: atoms, molecules” Publisher: Learning Development Institute (2012).
- [19] Eberhard Zeidler, “Quantum Field Theory II: Quantum Electro-dynamics”, Springer (2011).
- [20] Pople, J., and Beveridge, D., "Approximate Molecular Orbital Theory", McGraw – Hill (1970).
- [21] R. M. Dreizler, E. K. Gross, “Density Functional Theory”, Springer, (1990).
- [22] Robert G. Parr, Yang Weitao, “Density Functional Theory of atoms and molecules”, Oxford University press (1994).
- [23] L. H. Thomas, “The calculation of atomic fields”, Proc. Cambridge Philos. Soc. 23, 542 (1927).
- [24] P. Hohenberg, W. Kohn, “Inhomogeneous Electron Gas”, Phys. Rev. 136, B864 (1964).
- [25] W. Kohn, L. J. Sham, Phys. Rev. 140, A1133 (1965).
- [26] J. A. Pople and R. K. Nesbet, J. Chem. Phys. 22, 571 (1953).
- [27] R. Viswanatha, S. Sapra, T. S. Dasgupta and D. D. Sarma, Phys. Rev. B, Vol.72,2005, pp. 045333 (1-10); R. W. G. Wyckoff "Crystal Structures," Vol. 1, Interscience, New York, 2nd ed., 1963.
- [28] C. Allen, “Astrophysical quantities”, The Athlone Press (1973).
- [29] W. R. L. Lambrecht, O. K. Andersen, Phys. Rev. B 34, 2439 (1986).
- [30] R. Ahmed, Fazal-e-Aleem, S. J. Hashemifar, H. Rashid and H. Akbarzadeh, Communications in Theoretical Physics, Vol. 52, No. 3, 2009, pp. 527-533. doi:10.1088/0253-6102/52/3/28.
- [31] R. W. G. Wyckoff, “Crystal Structures,” 2nd Edition, R. E. Krieger, Malabar, 1986.
- [32] A. Aresti, L. Garbato and A. Rucci, J. Phys. Chem. Solids 45, 361 (1984).
- [33] A. S. VERMA, B. K SARKAR and V K JINDAL, journal of physics Vol. 74, No. 5,, May 2010 pp. 851–855.
- [34] N. H. Aysa, M. A. Abdulsattar, A.M. Abdul-ettif, Micro & Nano Letters 6, 137-140 (2011); M. A. Abdulsattar, K. H. Al-Bayati, Phys. Rev. B 75, 245201 (2007).
- [35] I. Vurgaftman, J. R. Meyer and L. R. Ram Mohan, J. appl. Phys. 89 (11) p. 5815 (2001).
- [36] M. Abdulsattar, Electronic Materials Letters , Vol 6, No.3(2010).
- [37] J.L. Powell, and B. Crasemann, "Quantum Mechanics", Addison-Wesley publishing company, INC. (1965).
- [38] G. Chen and A. Shakouri, "Transactions of the ASME", Vol.124, PP:242-252,(2005).
- [39] Charles Kittel, "Introduction to solid state physics", eighth edition, John Wiley and Sons (2005).